The monovalent cation leak in overhydrated stomatocytic red blood cells results from amino acid substitutions in the Rh-associated glycoprotein

Lesley J. Bruce,[1] Hélène Guizouarn,[2] Nicholas M. Burton,[1,3] Nicole Gabillat,[2] Joyce Poole,[1] Joanna F. Flatt,[1] R. Leo Brady,[3] Franck Borgese,[2] Jean Delaunay,[4] and Gordon W. Stewart[5]

[1]Bristol Institute for Transfusion Sciences, National Health Service Blood and Transplant, Bristol, United Kingdom; [2]Laboratoire de Biologie et Physiopathologie des Systèmes Intégrés, FRE3094 CNRS-Université de Nice, Nice, France; [3]Department of Biochemistry, University of Bristol, Bristol, United Kingdom; [4]Hématologie, Hôpital de Bicêtre, Assistance Publique-Hôpitaux de Paris; Faculté de Médecine Paris-Sud, Universite Paris-Sud, Inserm U779, Le Kremlin-Bicêtre, France; and [5]Department of Medicine, University College London, London, United Kingdom

Overhydrated hereditary stomatocytosis (OHSt) is a rare dominantly inherited hemolytic anemia characterized by a profuse membrane leak to monovalent cations. Here, we show that OHSt red cell membranes contain slightly reduced amounts of Rh-associated glycoprotein (RhAG), a putative gas channel protein. DNA analysis revealed that the OHSt patients have 1 of 2 heterozygous mutations (t182g, t194c) in *RHAG* that lead to substitutions of 2 highly conserved amino acids (Ile61Arg, Phe65Ser). Unexpectedly, expression of wild-type RhAG in *Xenopus laevis* oocytes induced a monovalent cation leak; expression of the mutant RhAG proteins induced a leak about 6 times greater than that in wild type. RhAG belongs to the ammonium transporter family of proteins that form pore-like structures. We have modeled RhAG on the homologous *Nitrosomonas europaea* Rh50 protein and shown that these mutations are likely to lead to an opening of the pore. Although the function of RhAG remains controversial, this first report of functional RhAG mutations supports a role for RhAG as a cation pore. (Blood. 2009;113:1350-1357)

Introduction

Overhydrated hereditary stomatocytosis (OHSt) was first reported in 1961[1] and has been extensively studied. The red cells have an invaginated cell shape suggestive of inward membrane bending. The red cells leak cations at a rate 20 to 40 times greater than normal and show a monotonic temperature dependence of the cation leak.[2] The massively increased permeability of these cells to the monovalent cations Na^+ and K^+ elicits a major increase in Na^+K^+-ATPase activity that in turn mandates an increase in glycolytic activity to provide ATP.[2] The cells have multiple abnormalities in the trafficking of membrane proteins, notably that of stomatin, a 32-kDa raft protein. Stomatin is lost from these cells as they mature,[3] and was named after this disease. Some patients with OHSt show subtle differences in red cell behavior. OHSt (type 1) ghost membranes show a defect in a process of ATP-dependent endocytic vesiculation that can be corrected by the cross-linker dimethyl adipimidate (DMA), which also corrects the cation leak in these cells.[4] OHSt (type 2) ghost membranes do not have the defect in ATP-dependent endocytic vesiculation, and the cation leak is not corrected by DMA.[4]

We were prompted to study the Rh-associated glycoprotein (RhAG) because we found that a related, less leaky condition known as cryohydrocytosis was caused by mutations in *SLC4A1*, which codes for the band 3 anion exchanger.[5] Band 3 is the focus of a macrocomplex of proteins that includes RhAG, and RhAG can be coimmunoprecipitated with anti–band 3 antibodies and thus associates directly with band 3.[6] Band 3 is involved in efficient red cell CO_2 transport, and the macrocomplex probably forms an integrated gas exchange metabolon[6]: however, the role of RhAG within the complex is not known. The function of RhAG is disputed, but it has been proposed that it may act as a gas channel or ammonium transporter because the Rh proteins form part of the ammonia transport (Amt) protein family. The crystallographic structures have been solved for certain Amt-like proteins, giving insight into the mechanism of ammonia transport. The first to be solved was for AmtB,[7,8] and more recently for the Rh50 protein from *Nitrosomonas europaea* (NeRh50),[9,10] which is a closer homolog of human RhAG (RhAG shares 20% sequence identity with AmtB and 36% with NeRh50). The structures of AmtB and NeRh50 are similar, with a root mean squared deviation of 1.4 Å over 268 aligned Cα atoms.[9] Both form trimers, with a hydrophobic pore through the center of each monomer. An unusual conserved twin-histidine motif protrudes into the center of the pore, which is otherwise entirely lined by hydrophobic residues. Entry to the pore from the extracellular vestibule in both AmtB and NeRh50 is restricted by the side chains of 2 conserved phenylalanine residues (the "phe-gate").

We have studied 7 OHSt kindreds (Table 1) and identified 2 novel heterozygous mutations (t182g, t194c) in *RHAG* leading to substitutions of 2 highly conserved amino acids (Ile61Arg, Phe65Ser). Expression in *Xenopus laevis* oocytes confirmed that the mutant RhAG proteins induced a large monovalent cation leak, and modeling of RhAG based on the homologous *N europaea* Rh50 protein structure suggested that these mutations lead to a more open pore structure.

Submitted July 25, 2008; accepted September 24, 2008. Prepublished online as *Blood* First Edition paper, October 17, 2008; DOI 10.1182/blood-2008-07-171140.

The online version of this article contains a data supplement.

The publication costs of this article were defrayed in part by page charge payment. Therefore, and solely to indicate this fact, this article is hereby marked "advertisement" in accordance with 18 USC section 1734.

Table 1. Genotype and phenotype of the OHSt kindreds

Pedigree/family code	Reference	Sex	Genotype	Phenotype
Stockport				
A-I-1	1, 11	M	Phe65/Phe65	Unaffected
A-I-2		F	Phe65/Ser65	OHSt
A-II-1*†		M	Phe65/Ser65	OHSt
A-II-2		F	Phe65/Ser65	OHSt
A-III-1		F	Not tested	OHSt
A-III-2		M	Phe65/Phe65	Unaffected
Albuquerque				
C-I-1	12	M	Not tested	—
C-I-2*†		F	Phe65/Ser65	OHSt
C-II-1		M	Phe65/Ser65	OHSt
C-II-2		F	Phe65/Ser65	OHSt
Brighton				
B-II-1†	11, 13	F	Phe65/Ser65	OHSt
B-III-1		M	Phe65/Phe65	Unaffected
Toulouse				
B-I-1	12	M	Phe65/Phe65	Unaffected
B-I-2		F	Phe65/Phe65	Unaffected
B-II-1		M	Phe65/Ser65	OHSt
Grenoble				
A-I-1	14	M	Deceased	OHSt
A-I-2		F	Not tested	Unaffected
A-II-1		M	Phe65/Ser65	OHSt
A-III-1		F	Phe65/Ser65	OHSt
Nancy				
—	—	M	Phe65/Ser65	OHSt
Harrow				
A-II-3*†	12	F	Ile61/Arg61	OHSt

**RHAG* analyzed by SSCP (OHSt samples from Montpellier[12] and San Francisco[12] were also analyzed but no mutations found. OHSt in these 2 cases is part of a more complex picture, including neurologic symptoms, and thus has a different genetic origin; OMIM 608885; http://www.ncbi.nlm.nih.gov).

†All 10 exons of *RHAG* DNA were sequenced.

Methods

Patients

All patients had classical OHSt with very leaky red cells (Na^+ and K^+ transport rates of about 40 times that of normal at 37°C) resulting in moderate hemolytic anemia.[2] Mean red cell volumes were abnormally large (approximately 140 fL), and blood smears showed the presence of stomatocytes, echinocytes, target cells, macrocytes, and (if splenectomized) punctate red cells. Osmotic ektacytometry displayed a shifted curve typical in OHSt (Figure S1, available on the *Blood* website; see the Supplemental Materials link at the top of the online article). Patients are designated by their place of origin and their position in the family (Table 1). Some pedigrees have been reported previously.[1,11-14] The male patient "OHSt Nancy," who was born in 1987, is described in Figure S1. Patient blood samples were collected and informed consent was obtained in accordance with the Declaration of Helsinki. The red cell protein and DNA analysis are diagnostic, both extending and refining the diagnosis of the disease phenotype.

Serologic tests

Plasma was tested for antibody specificity using standard serologic indirect antiglobulin test (IAT) tests using both tube and gel techniques and untreated and papain-treated cells. Red cells were tested for selected high-incidence antigens.

Red cell membrane protein analysis

Preparation of red cell membranes, SDS-PAGE, Coomassie blue staining, and Western blotting of membrane proteins were carried out as previously described.[6] Protein concentration was estimated using the Bradford assay and equal amounts (typically 10 μg) of ghosts loaded per track of each gel. The rabbit antipeptide antibodies anti-RhAG, anti-Rh, anti-CD47, and anti-stomatin were used as previously described.[6]

Analysis by SSCPs and DNA sequencing

Genomic DNA was isolated from blood samples. The coding regions of exons 1 to 10 of human *RHAG*[15,16] were analyzed for single-strand conformation polymorphisms (SSCPs) using exon-specific primers. All altered or anomalous banding patterns were further investigated by DNA sequencing as described previously.[5] DNA sequencing was used to analyze exon 2 of *RHAG* from all available family members and 56 unrelated controls.

Preparation of mutant constructs and expression in *Xenopus laevis* oocytes

The cDNA clones in *X laevis* expression vector BSXG1 encoding human RhAG (BSXG1.RHAG) and glycophorin B (BSXG.GPB) have been described.[17] They contain the cDNAs encoding human intact red cell RhAG and GPB, respectively, flanked by the 5′ and 3′ noncoding regions of *Xenopus* β-globin. Amino acid substitutions Phe65Ser and Ile61Arg were made using the Quikchange II mutagenesis kit (Strategene, Amsterdam Zuidoost, The Netherlands) using BSXG1.RHAG as a template and the following primers: I61R sense ccaagatgtacatgttatgagatttgttgggtttggcttcc, I61R antisense ggaagccaaacccaacaaatctcataacatgtacatcttgg, F65S sense agatgtacatgttatgatatttgttgggtctggcttcctcatgac, and F65S antisense gtcatgaggaagccagacccaacaaatatcataacatgtacatct.

The sequences of the final constructs were confirmed by automated sequencing (ABI PRISM 3100 Genetic Analyzer Automatic Sequencer; Applied Biosystems, Courtaboeuf, France). The methods used for the preparation of cRNA, expression in oocytes, and measurement of Na^+ and K^+ content by flame photometry have been described.[5] Glycophorin B is thought to increase the expression of RhAG at the plasma membrane,[18] and was coinjected (2.5 ng) with the wild-type (10 ng) or mutant (10 ng) RhAG. After injection, oocytes were kept at 19°C in modified Barth saline (MBS) composed of 85 mM NaCl, 1 mM KCl, 2.4 mM $NaHCO_3$, 0.82 mM $MgSO_4$, 0.33 mM $Ca(NO_3)_2$, 0.41 mM $CaCl_2$, 10 mM HEPES, and 4.5 mM NaOH (pH 7.4) supplemented with penicillin (10 U/mL) and streptomycin (10 μg/mL). Oocytes dedicated to Na^+ and K^+ content measurements were incubated following injection at 19°C for 2 or 3 days in MBS with ouabain (0.5 mM) and bumetanide (5 μM) to prevent any Na^+ or K^+ recycling or movement through the Na^+/K^+ pump or Na^+-K^+-$2Cl^-$ cotransporter. After incubation 5 oocytes were quickly rinsed twice in milliQH_2O and dried overnight at 80°C. Each condition and experiment was done in triplicate.

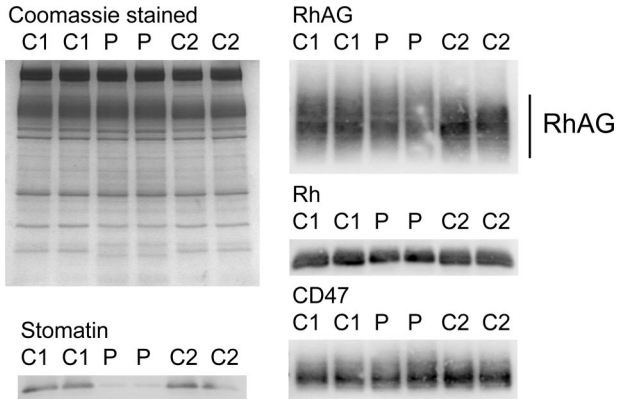

Figure 1. Red cell membrane protein analysis. Red cell membranes were separated on 10% Laemmli gels and Coomassie stained or immunoblotted using antibodies as shown. Loading: C1, C2, controls 1 and 2. P indicates proband (Stockport A-II-1). The RhAG is heavily glycosylated (seen as a broad 50- to 80-kDa band). In the proband, the amount of RhAG was reduced and the band was slightly shifted, suggesting hyperglycosylation. The Rh polypeptides were also reduced in expression, in proportion to the reduction of RhAG. CD47 appears unchanged. The reduction in stomatin has been shown previously and is characteristic of OHSt.

Intracellular cations were extracted from dried oocytes by overnight incubation in 4 mL milliQH_2O. Na^+ and K^+ were quantified by flame photometry (Eppendorf, Le Pecq, France).

Li influx measurements

Li^+ was used as a substitute for Na^+ to measure oocyte cation permeability. NO_3^- containing medium was used to avoid any involvement of cation movements through the KCl cotransporter (Li^+ influx was not significantly different when measured in MBS where NaCl was substituted with $LiNO_3$ or with LiCl). Oocytes (7 per condition) were incubated for 2 hours at 19°C in MBS, where NaCl was substituted by $LiNO_3$. Composition was as follows: 85 mM $LiNO_3$, 1 mM KNO_3, 2.4 mM $KHCO_3$, 0.82 mM $MgSO_4$, 0.33 mM $Ca(NO_3)_2$, 0.41 mM $CaCl_2$, 10 mM HEPES, and 4.5 mM NaOH (pH 7.4). In addition, ouabain (0.5 mM) and bumetanide (5 μM) were added to block the Na^+/K^+ pump and the Na^+-K^+-$2Cl^-$ cotransporter, respectively. Incubation for 2 hours was within the linear phase of Li influx. Oocytes were washed 3 times in milliQH_2O and placed one by one in a tube heated at 95°C to desiccate. Intracellular Li^+ was extracted by addition of 50 μL 0.1 N NaOH and further diluted by addition of 250 μL milliQH_2O. The Li^+ content in each oocyte extract was measured by atomic absorption spectrometry with a PerkinElmer 3110 (PerkinElmer SAS, Courtaboeuf, France).

Immunoblotting of expressed protein

Oocyte membranes were prepared as described previously,[19] resuspended in 20 mM Tris HCl buffer (pH 7.4), 250 mM sucrose, and 8 M urea with protease inhibitor Pefabloc (Roche, Meylan, France) and heated for 15 minutes at 37°C. The membranes were mixed with loading buffer containing DTT and run on an 8% SDS-PAGE polyacrylamide gel. Western blots were incubated with a rabbit antipeptide RhAG antibody (as in "Red cell membrane protein in analysis", 1:1000) in Tris-buffered saline, 0.1% Tween-20 with 1% fat-free dry milk powder (wt/vol). The secondary antibody was a goat IgG-peroxydase (Sigma, Lyons, France) used at 1:80 000 dilution. The signal was visualized by enhanced chemiluminescence (PerkinElmer SAS) and Kodak Biomax film (Sigma).

Structural modeling of the mutant RhAG proteins

The crystallographically determined structure of NeRh50 (Protein Data Bank [PDB] ID 3B9W)[9] was used as a template to build homology models of RhAG and the Rh polypeptides using the MODELLER software.[20] Models were optimized using a thorough variable target function optimization and 300 cycles of simulated annealing molecular dynamics. The process was repeated to generate 20 models for each of the wild-type and OHSt mutant RhAG proteins. For each protein, the model with the lowest objective function was selected for further analysis. The quality of each model was assessed with PROCHECK[21] and MOLPROBITY.[22] For all the models, no less than 95% of residues lay in the most favored regions of the Ramachandran plot, and all other stereochemical parameters were within expected ranges.

Results

Red cell membrane protein analysis

SDS-PAGE and Coomassie staining of OHSt red cell membranes (Table 1; Stockport A-II-1) revealed the reduction in stomatin, as

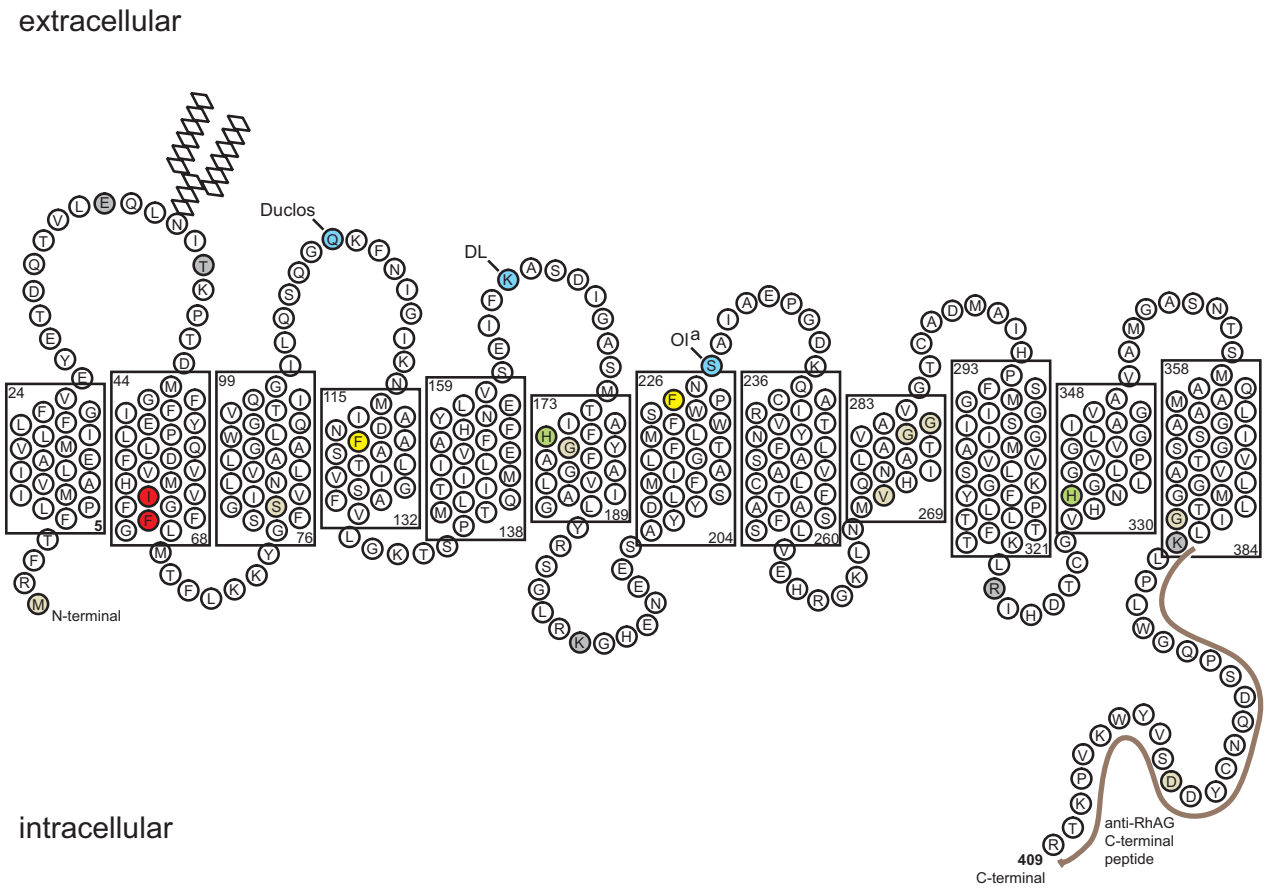

Figure 2. Schematic model of RhAG. The 2-D model shows the RhAG protein with transmembrane spans as predicted by the alignment of RhAG with NeRh50.[9] The layout emphasizes the close proximity of the 2 residues associated with OHSt, Ile61 and Phe65, found in span 2 and highlighted in red. The phenylalanines that form the putative phe-gate (Phe120 and Phe225) are highlighted in yellow. The 2 highly conserved His residues (His175 and His334) are highlighted in green. Beige infill denotes residues mutated in Rh_{null} syndrome. Frame shift and splice site mutations have also been reported in Rh_{null} (reviewed in Bruce[23]; data not shown). Blue infill denotes blood group sites that have been assigned to RhAG very recently.[24] Gray infill denotes sites susceptible to proteolytic cleavage.[25] The C-terminal peptide, used in preparation of the anti-RhAG antibody, is marked by a brown line.

```
Caenorhabditis elegans 1     NP_504436.1 THVMIFIGFGFLMTFLKRYGFSAVSINMLLAVFTIQWGIIV
Caenorhabditis elegans 2     NP_505961.1 VHLMIFVGFGFLMAFLKRYGFSAVSVNLLLSAFVIQFAMLL
Ambystoma tigrinum tigrinum   AAV28818.1 VHVMIFIGFGFLMTFLKRYGFSSVGINLLIAALGLQWGTLM
Xenopus laevis              NP_001081429 VHVMIFVGFGFLMTFLKRYGFSSVGVNMLIAALGLQWGILM
Gasterosteus aculeatus        ABF69688.1 VHVMIFIGFGFLMTFLKRYGFSSVGFNLLLAAFGLQWGLLT
Takifugu rubripes          NP_001032956.1 VHVMIFIGFGFLMTFLKRYGFSSVGVNLLLAAFGLQWGLLM
Oncorhynchus mykiss           ABV24962.1 VHVMIFIGFGFLMTFLKRYGFSSVGLNLLLAAFALQWGLIM
Danio rerio                  NP_998010.1 VHVMIFIGFGFLMTFLKRYGFTSVGVNLLLAAFGLQWGLLL
Bos taurus                   NP_776596.1 VHIMVFAGFGFLMTFLWKYGFSGVGINLLIAALGLQWGTII
Equus caballus              XP_001498649 VHVMVFIGFGFLMTFLKNYGFGGVSFNLFIAALGLQCGIMA
Gorilla gorilla               AAG00304.1 VHVMIFVGFGFLMTFLKKYGFSSVGINLLVAALGLQWGTIV
Homo sapiens                 NP_000315.2 VHVMIFVGFGFLMTFLKKYGFSSVGINLLVAALGLQWGTIV
Pan troglodytes            NP_001009033.1 VHVMIFVGFGFLMTFLKKYGFSSVGINLLIAALGLQWGTIV
Hylobates sp                  AAG00306.1 VHVMIFVGFGFLMTFLKKYGFSSVGINLLVAALGLQWGTIV
Pongo pygmaeus                AAG00305.1 VHVMIFVGFGFLMSFLKKYGFSSVGINLLIAALGLQWGTIV
Macaca fascicularis           BAA32444.1 VHVMIFVGFGFLMTFLKKYSFSSVGINLLIAALGLQWGTVV
Papio hamadryas               AAG00308.1 VHVMIFVGFGFLMTFLKKYGFSSVGINLLIAALGLQWGTVV
Macaca mulatta             NP_001027987.1 VHVMIFVGFGFLMTFLKKYGFSSVGINLLIAALGLQWGTVV
Cebus apella                  AAF37156.1 VHVMIFVGFGFLMTFLKKYGFSSVGFNLLIAALGLQWGTIA
Mus musculus                 NP_035399.1 VHVMIFVGFGFLMTFLKKYGFSGVGFNLFLAALGLQWGTIM
Rattus norvegicus            NP_075411.2 VHVMIFVGFGFLMTFLKKYGFSGVGFNLFLAALGLQWGTIV
Canis lupus familiarus       NP_001104238 VHVMIFVGFGFLMTFLKKYGFSSVGINLLIAALGLQWGTFV
Monodelphis domestica        XP_001369635 VHVMIFTGFGFLMTFLKKYGFSSVGINLMIAALGLQWGTFM
Ornithorhynchus anatinus     XP_001510671 VHVMIFIGFGFLMTFLKKYGFSSVGFNLLIAALGLQWGTLM
Gallus gallus                 NP_989795.1 VHVMIFIGFGFLMTFLKKYGFTSVGINMLIAAFGLQWGTLM
Kryptolebias marmoratus       ABD83662.1 VHVMIFVGFGFLMTFLKRYSYGGVGFNFLIASFGLQWALLM
Oryzias latipes               BAB13346.1 VHVMIFVGFGFLMTFLKRYSFSAVGFNFLIAAFGLQWALLM
Tetraodon nigroviridis        CAG04561.1 VHVMIFIGFGFLMTFLQKYGFGSVGFNFLIAAFSLQWATLM
Takifugu rubripes 1        NP_001027816.1 VQVMIFIGFGCLLAFFRFYGFSGMVFNFLTATFTIQWAILV
Takifugu rubripes 2        NP_001027817.1 IQVMIFIGFGCLLAFFRLYGFGGMAFNFLMATFAIQWAILV
Geodia cydonium               CAA73029.1 VHVMIFVGFGFLMTFLRRYGFGSISFNLLLASFAIQWSTLT
Ciona intestinalis         NP_001027948.1 VHVMIFIGFGFLMTFLKRYGFGSVGFNFMLAAFVIQWTILM
Drosophila melanogaster       NP_647940.1 IQVMIFIGFGFLMTFLRKYGYSATGFTLFMAALVVQWAVLM
Dictyostellum discoideum      XP_641341.1 ININIFFGFGFLMTFLRRYGYSALGYTFIISALVAQWSVLI
Chlamydomonas reinhardtii       AAK14648 VNIMVWIGFGFLMTFMRRYGYGAVALNYFASALMFLEAILM
Chlamydomonas reinhardtii 2 XP_001695465 VQVMIFIGFGFLMTFMRRYSYGAVSLNYFASALMFLEAILM
Nitrosomonas europaea         AAR24581.1 ILAMLLVGFGFLMVFVRRYGFSATTGTYLVVATGLPLYILL
                                          *:  *** *: *.  *.: .   . :          .
```

Figure 3. Multiple DNA sequence alignment of RhAG proteins. A total of 37 RhAG and RhAG-like protein sequences were aligned using EMBL-EBI CLUSTALW (EMBL-EBI, Cambridge, United Kingdom) from sequences identified using the National Center for Biotechnology Information (NCBI, Bethesda, MD) Human Genome Resources and BLASTP. The species' name, protein number, and a portion of the sequence are shown (amino acids 59-102 of the human sequence). Amino acids 61 and 65 (of the human sequence) are boxed, showing that Ile61 is conserved and Phe65 is identical across all 37 sequences. This figure shows only a fragment of the RhAG protein sequence; a complete alignment of 111 Rh sequences can be found in the supporting information of Huang and Peng.[26]

described previously,[1,11] but no other obvious changes in the major membrane proteins (Figure 1). However, immunoblotting analysis showed the RhAG protein from OHSt red cells was expressed at slightly lower levels and displayed altered electrophoretic mobility (Figure 1). The Rh polypeptides were likewise reduced, reflecting their dependence on RhAG for stable expression in the red cell membrane; CD47, however, was not noticeably altered (Figure 1).

DNA analysis

These alterations in the RhAG protein prompted us to examine the *RHAG* gene in patients with OHSt. SSCP analysis showed 2 different band shift patterns in exon 2, and DNA sequencing identified 2 heterozygous mutations (t182g, t194c) in *RHAG* leading to substitutions of amino acids Ile61Arg and Phe65Ser, respectively. The Phe65Ser mutation was associated with OHSt in 6 kindreds (OHSt type 1) and Ile61Arg in 1 (OHSt type 2; Table 1; Figure 2). To check that these novel mutations were not simply single-nucleotide polymorphisms, we sequenced the DNA from 56 unrelated control DNAs (112 alleles), all coded for the normal RhAG protein. Amino acids 61 and 65 are within a highly conserved region of the RhAG protein. Ile61 is conserved and Phe65 is identical across 37 RhAG or RhAG-like protein sequences[26] (Figure 3) and across 39 RhBG or RhCG protein sequences, the nonerythroid homologs of RhAG.[26]

Cation transport in oocytes

To investigate the cation transport properties of the mutant RhAG proteins when expressed in a heterologous system, we injected *X laevis* oocytes with cRNA coding for wild-type RhAG, Ser65-RhAG, or Arg61-RhAG. Both wild-type and mutant RhAG proteins were substantially expressed at the oocyte membrane (Figure 4A). We measured both Li^+ uptake (Figure 4B) and the levels of intracellular Na^+ and K^+ after 2 (Figure 4C) and 3 (Figure 4D) days. In the presence of a monovalent cation leak, internal $[Na^+]$ will rise and $[K^+]$ will fall.[5] Unexpectedly, expression of wild-type RhAG led to an increase in Li^+ uptake, a rise in intracellular $[Na^+]$, and a fall in intracellular $[K^+]$, such that after 3 days, intracellular $[Na^+]$ exceeded intracellular $[K^+]$ (Figure 4D). When the mutants Ser65-RhAG or Arg61-RhAG were expressed, Li^+ uptake was about 6 times that seen with wild-type, and the intracellular Na^+ and K^+ levels were very markedly abnormal (Figure 4B,C); after

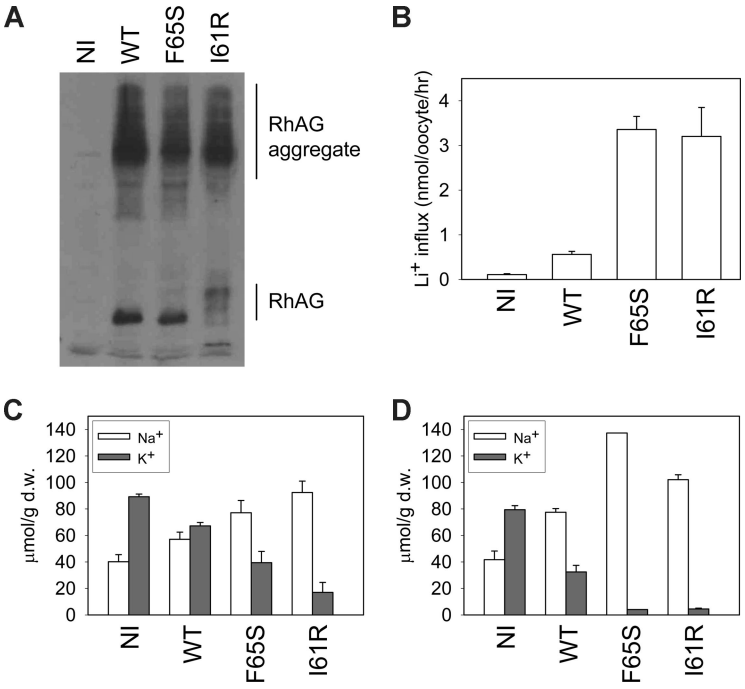

Figure 4. Cation leak in *X laevis* oocytes expressing wild-type or mutant RhAG. (A) RhAG expression levels in *X laevis* oocytes were assessed by immunoblotting using an antibody to C-terminal RhAG. A proportion of aggregate was detected, as indicated. (B) Li^+ uptake (as a surrogate for Na^+) was measured 2 days after injection. The result is a representative experiment of 4 repeats. Data are means of 7 oocytes plus or minus SEM. (C) Intracellular sodium and potassium ion concentrations were measured 2 days after injection. Data, expressed in micromolar per gram of dry weight (µmol/g d.w.), are the mean values for 3 separate experiments plus or minus SEM. (D) Intracellular sodium and potassium ion concentrations were measured 3 days after injection. Data, expressed in micromolar per gram of dry weight, are the means of triplicate measurements for each condition plus or minus SEM. The result is a continuation of one of the experiments shown in panel C.

3 days of incubation, intracellular [Na^+] hugely exceeded intracellular [K^+], which was barely detectable (Figure 4D). These changes exactly mimic those seen on OHSt red cells,[2] and strongly support the contention that it is the mutated RhAG that mediates the cation leak in these cells.

RhAG modeling

We used the NeRh50 structure as a template to construct models of the wild-type and mutant RhAG proteins (Figure 5; Document S1 and Figure S2 show a more detailed description of the RhAG model). Our model of wild-type human RhAG shows no major structural changes compared with NeRh50. In the central pore region, both the twin-histidine motif (His175 and His334 in RhAG) and the phe-gate (Phe120 and Phe225 in RhAG) are conserved (Figure 5A-C,F). At the cytoplasmic end of the pore there is a constriction formed by His334 of the conserved pair and by Phe65. Mutation of Phe65 to serine, as found in the patients with type 1 OHSt, alters this constriction, opening the pore from the cytoplasmic surface to the phe-gate (Figure 5D,G). The modeling predicts a minimum pore diameter of approximately 3.6 Å for Ser65-RhAG, which is larger than the hydrated radii of Na^+ (3.58 Å), K^+ (3.31 Å), and NH_4^+ (3.31 Å).[27] Our model of the Ile61Arg mutant of RhAG predicts small, local, structural changes, which again result in the opening up of the central pore region (Figure 5E,H). In this case, the minimum pore diameter observed in the model is 1.5 Å. However, incorporation of the positively charged guanidinium group from the arginine into a hydrophobic region (Figure 5E,H) may lead to more pronounced structural changes. Both models predict that the OHSt mutations will result in the phe-gate being the major barrier to the passage of substrate through the central pore. Opening of the phe-gate appears to be a prerequisite for the passage of substrate through all AmtB and Rh50 proteins.[7,9] The phe-gate could be opened by a simple rotation of the side-chain of the C-terminal phenylalanine without any major structural rearrangement (Document S1).

Serologic analysis

One patient (Table 1; Stockport A-II-2) had received transfusions multiple times, and it became increasingly difficult to find compatible blood. Anti-c was identified in the plasma and an additional, weaker antibody that reacted with all normal red cell samples. The patient's red cells were positive with a range of antibodies to high-incidence antigens. The only cells that were compatible with the plasma were Rh_{null} cells (3 examples) and those of the patient's affected brother (Table 1; Stockport A-II-1). D- - cells were weakly reactive. Compatibility with the cells of the patient's brother suggested that their red cells lacked the same epitope, although no antibody was detectable in his plasma. The compatibility with Rh_{null} cells, that lack not only RhAG but also the Rh polypeptides and CD47, suggested that the epitope was formed against one of the proteins of the Rh complex. Both the patient's and the brother's red cells had normal Rh antigens (R1R1); therefore, the Rh polypeptides were present. Immunoblotting showed normal amounts of CD47 (Figure 1). D- - cells contain reduced amounts of RhAG (J.F.F., L.J.B., unpublished results, July 2008), and thus these data suggested that this weak antibody was formed against an epitope on RhAG.

Discussion

We have shown in this paper that mutations in *RHAG* cause OHSt, and that the large cation leak in OHSt red cells is almost certainly carried by the mutant RhAG proteins. Interestingly, we have also found that wild-type RhAG leaks monovalent cations. The physiologic function of RhAG is disputed. Its homology to the Amt proteins suggests that it may act as a cation channel transporting NH_4^+, or as a gas channel moving NH_3 or CO_2. However, early studies of the transport properties of human RhAG gave conflicting results, variously describing RhAG as a NH_3/NH_4^+ exchanger or ammonium transporter,[28-31] or as an ammonia channel,[32-34] or suggesting that RhAG transports CO_2,[35] or both CO_2 and NH_3.[36]

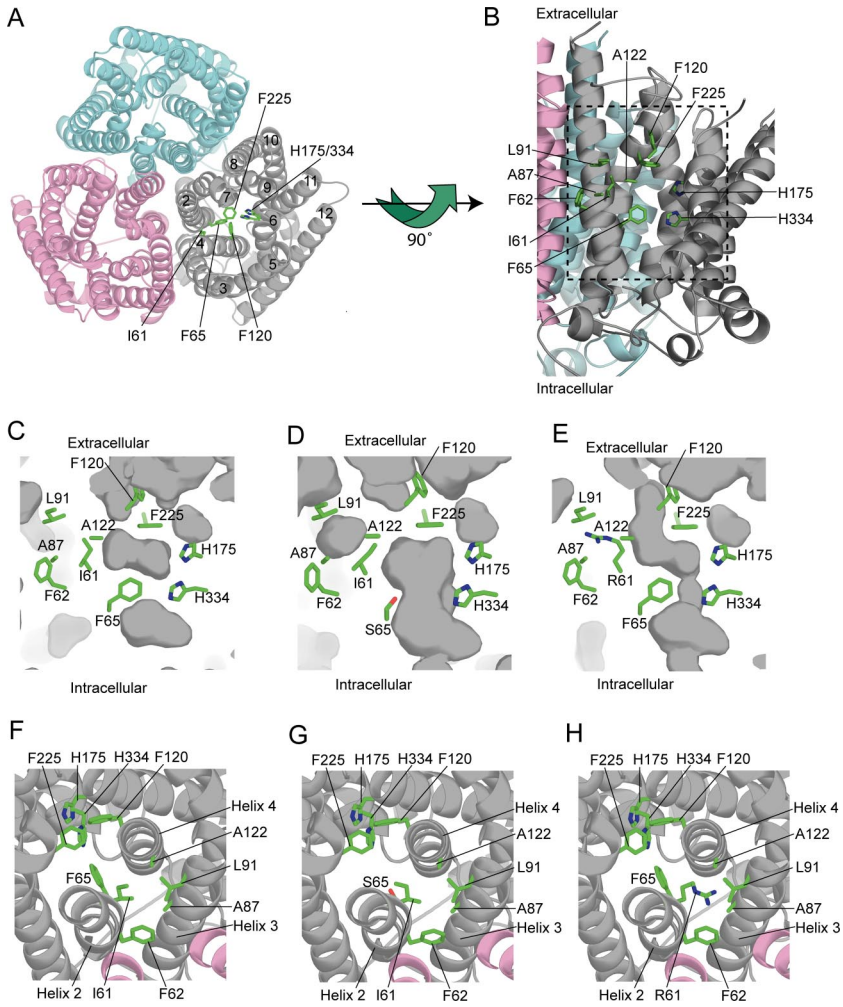

Figure 5. Homology model of RhAG. (A) Structural model of the RhAG trimeric complex looking from the outside of the cell. The helices 2 through 12 are displayed as Cα ribbon and are numbered for one RhAG monomer. The twin-histidine motif (His175 and His334), the phe-gate (Phe120 and Phe225), and residues mutated in OHSt patients (Ile61 and Phe65) are labeled. (B) Side view of the channel in one monomer of wild-type RhAG. Helices 3, 4, and 5 of the gray monomer have been removed to show the putative conductance pathway. In addition to the residues labeled in panel A, side-chains of residues that contribute to the hydrophobic environment of the Ile61 side-chain are marked. The dashed box indicates the area displayed in panels C through E. (C) Close-up view of the central pore in one monomer of wild-type RhAG. A cross-section of the central pore of one monomer of wild-type RhAG is shown. The protein surface is colored gray, with darker areas representing either solvent accessible surface or cavities within the protein. Side-chains of key residues are shown and labeled as in panel B. (D) Close-up view of the central pore in one monomer of Ser65 RhAG. A cross-section of the central pore of one monomer of Ser65 RhAG is shown and labeled as in panel B. The replacement of Phe65 with Ser65 is predicted to open the pore structure to a minimum width of about 3.6 Å between the cytoplasm and the phe-gate. This is sufficiently wide to allow hydrated Na^+ (3.58 Å), K^+ (3.31 Å), and NH_4 (3.31 Å) ions to pass.[27] (E) Close-up view of the central pore in one monomer of Arg61 RhAG. A cross-section of the central pore of one monomer of Arg61 RhAG is shown and labeled as in panel B. The replacement of Ile61 with Arg61 is predicted to open the pore structure to a minimum width of about 1.5 Å between the cytoplasm and the phe-gate. However, the incorporation of the positively charged guanidinium group from the arginine into a hydrophobic region may lead to more pronounced structural changes than those observed in our model. (F) The central pore of one monomer of wild-type RhAG looking from the outside of the cell. The wild-type model is viewed looking down through the central pore. The model is colored and labeled as in panel B. (G) The central pore of one monomer of Ser65 RhAG looking from the outside of the cell. The Ser65 model is viewed looking down through the central pore. Replacement of Phe65 with Ser65 opens up the pore structure beyond the phe-gate. The model is colored and labeled as in panel B. (H) The central pore of one monomer of Arg61 RhAG looking from the outside of the cell. The Arg61 model is displayed showing the hydrophobic environment of the Arg61 side-chain and its relationship to the central pore. The model is colored and labeled as in panel B.

Recently, even the gas channel hypothesis has been disputed.[37] This is the first study to show that wild-type RhAG can act as a pore for other monovalent cations (Na^+, K^+, Li^+), at least when expressed in *X laevis* oocytes. Interestingly, a recent study has shown that AmtB allows accumulation of methylammonium cations in response to variation in the electrical potential across the bacterial membrane.[38] These authors also showed that the rate of flux of methylammonium through an AmtB mutant (Trp148Leu), predicted to enlarge the AmtB pore, was about 10 times faster than through wild-type AmtB.[38] Modifying their own previous conclusions, these authors inferred that AmtB can act as an ion channel.[38] Similarly, we find that RhAG can mediate a basal cation flux, the rate of which is increased by mutations that are predicted to open the pore structure.

Two observations suggested that the Phe65Ser mutation not only alters the pore structure but also causes long-range structural alterations in RhAG. The first involved a patient (Table 1; Stockport A-II-2) who had made an antibody against a RhAG epitope. Since in this heterozygous condition both the wild-type and Ser65-RhAG proteins should be present, the altered epitope was probably formed by changes in the oligomeric interactions of RhAG, and suggests that WT-RhAG forms hetero-oligomers with Ser65-RhAG. Another observation indicating long-range structural alterations was the inhibitory effect of DMA on these Phe65Ser RhAG cells,[4] suggesting that the position or orientation of extracellular lysine residue(s) are altered in the Phe65Ser RhAG, creating a DMA binding site that is not found in wild-type or I61R RhAG.

OHSt cells are deficient in the raft protein stomatin, and stomatin expression is also reduced in a subtype of cryohydrocytosis.[12] However, no mutation was found in either *SLC4A1* or *RHAG* for this condition (Table 1). Both this subtype and OHSt have exceptionally leaky red cells, and we have previously suggested that the loss of stomatin in these cells may be linked to glycolytic activity.[12] It has more recently been shown that stomatin may act as a molecular switch that, when present, converts the glucose transporter Glut1 (SLC2A1) into a transporter of L-dehydroascorbic acid, an oxidized form of ascorbic acid.[39] If stomatin is absent, Glut1 acts as a glucose transporter. Thus, the loss of stomatin from these cells may well be triggered by the need for increased glycolysis required to fuel the increased Na^+K^+-ATPase activity[40] demanded by the cation leak. The mechanism of this regulation has yet to be defined.

The data here show unequivocally that OHSt is caused by mutations in *RHAG*. We have shown that wild-type RhAG protein induces a cation flux when expressed in *X laevis* oocytes, while the mutants induce a much larger flux. Modeling studies indicate that both mutations dilate a cytoplasmic constriction in the RhAG pore. Together, these data suggest that wild-type RhAG has the properties of a cation pathway. It is possible that in its natural environment, as part of the band 3 macrocomplex, RhAG forms a regulated cation channel that is only active under certain conditions. This is the first report of mutant RhAG proteins with any measurable physiologic activity: all previous *RHAG* mutations have been recessive and have resulted in the Rh_{null} phenotype. Further study of the present mutants may help reveal the true function of RhAG.

Acknowledgments

We thank Peter Martin for DNA sequencing; Dr Thérèse Cynober for performing osmotic gradient ektacytometry; Dr Corinne Armari-Alla, Dr Alain Robert, and Prof Danièle Sommelet for providing patient blood samples; and Dr Stuart Winter and Dr Cecil Reid for permission to report their patients. We thank all of the patients for their cooperation.

This work was supported by the UK National Health Service R&D Directorate (L.J.B., J.F.F.). N.M.B. was supported by a studentship from the UK Medical Research Council. G.W.S. thanks Advocacy for Neuroacanthocytosis for generous funding.

Authorship

Contribution: L.J.B. conceived the original hypothesis, performed research design and protein and DNA analysis, and prepared the manuscript; H.G., F.B., and N.G. performed expression studies in *X laevis* oocytes; N.M.B. and R.L.B. performed modeling studies and prepared the manuscript; J.P. performed serology; J.F.F. performed immunoblotting; and J.D. and G.W.S. provided patient samples and prepared the manuscript.

Conflict-of-interest disclosure: The authors declare no competing financial interests.

Correspondence: Lesley Bruce, Bristol Institute for Transfusion Sciences, NHS Blood and Transplant, North Bristol Park, Filton, Bristol, BS34 7QH, United Kingdom; e-mail: lesley.bruce@nhsbt.nhs.uk.

References

1. Lock SP, Sephton Smith R, Hardisty RM. Stomatocytosis: a hereditary haemolytic anomaly associated with haemolytic anaemia. Br J Haematol. 1961;7:303-314.
2. Stewart GW. Hemolytic disease due to membrane ion channel disorders. Curr Opin Hematol. 2004;11:244-250.
3. Fricke B, Parsons SF, Knöpfle G, von Düring M, Stewart GW. Stomatin is mis-trafficked in the erythrocytes of overhydrated hereditary stomatocytosis, and is absent from normal primitive yolk sac-derived erythrocytes. Br J Haematol. 2005; 131:265-277.
4. Turner EJ, Jarvis HG, Chetty MC, et al. ATP-dependent vesiculation in red cell membranes from different hereditary stomatocytosis variants. Br J Haematol. 2003;120:894-902.
5. Bruce LJ, Robinson HC, Guizouarn H, et al. Monovalent cation leaks in human red cells caused by single amino-acid substitutions in the transport domain of the band 3 chloride-bicarbonate exchanger, AE1. Nat Genet. 2005;37:1258-1263.
6. Bruce LJ, Beckmann R, Ribeiro ML, et al. A band 3–based macrocomplex of integral and peripheral proteins in the RBC membrane. Blood. 2003;101: 4180-4188.
7. Khademi S, O'Connell J 3rd, Remis J, Robles-Colmenares Y, Miercke LJ, Stroud RM. Mechanism of ammonia transport by Amt/MEP/Rh: structure of AmtB at 1.35 A. Science. 2004;305: 1587-1594.
8. Zheng L, Kostrewa D, Bernèche S, Winkler FK, Li XD. The mechanism of ammonia transport based on the crystal structure of AmtB of Escherichia coli. Proc Natl Acad Sci U S A. 2004;101:17090-17095.
9. Lupo D, Li XD, Durand A, et al. The 1.3-Å resolution structure of *Nitrosomonas europaea* Rh50 and mechanistic implications for NH3 transport by Rhesus family proteins. Proc Natl Acad Sci U S A. 2007;104:19303-19308.
10. Li X, Jayachandran S, Nguyen HH, Chan MK. Structure of the *Nitrosomonas europaea* Rh protein. Proc Natl Acad Sci U S A. 2007;104:19279-19284.
11. Fricke B, Argent AC, Chetty MC, et al. The "stomatin" gene and protein in overhydrated hereditary stomatocytosis. Blood. 2003;102:2268-2277.
12. Fricke B, Jarvis HG, Reid CD, et al. Four new cases of stomatin-deficient hereditary stomatocytosis syndrome: association of the stomatin-deficient cryohydrocytosis variant with neurological dysfunction. Br J Haematol. 2004;125:796-803.
13. Meadow SR. Stomatocytosis. Proc R Soc Med. 1967;60:13-15.
14. Morle L, Pothier B, Alloisio N, et al. Reduction of membrane band 7 and activation of volume stimulated (K^+, Cl^-)-cotransport in a case of congenital stomatocytosis. Br J Haematol. 1989;71: 141-146.
15. Ridgwell K, Spurr NK, Laguda B, MacGeoch C, Avent ND, Tanner MJ. Isolation of cDNA clones for a 50 kDa glycoprotein of the human erythrocyte membrane associated with Rh (rhesus) blood-group antigen expression. Biochem J. 1992;287:223-228.
16. Huang C-H. The human Rh50 glycoprotein gene: structural organization and associated splicing defect resulting in Rh_{null} disease. J Biol Chem. 1998;273:2207-2213.
17. Young MT, Tanner MJ. Distinct regions of human glycophorin A enhance human red cell anion exchanger (band 3; AE1) transport function and surface trafficking. J Biol Chem. 2003;278:32954-32961.
18. Ridgwell K, Eyers SA, Mawby WJ, Anstee DJ, Tanner MJ. Studies on the glycoprotein associated with Rh (rhesus) blood group antigen expression in the human red blood cell membrane. J Biol Chem. 1994;269:6410-6416.
19. Martial S, Guizouarn H, Gabillat N, Pellissier B, Borgese F. Importance of several cysteine residues for the chloride conductance of trout anion exchanger 1 (tAE1). J Cell Physiol. 2007;213:70-78.
20. Sali A, Blundell TL. Comparative protein modelling by satisfaction of spatial restraints. J Mol Biol. 1993;234:779-815.
21. Laskowski RA, MacArthur MW, Moss DS, Thornton JM. Procheck: a program to check the stereochemical quality of protein structures. J Appl Crystallog. 1993;26:283-291.
22. Davis IW, Murray LW, Richardson JS, Richardson DC. MOLPROBITY: structure validation and all-atom contact analysis for nucleic acids and their complexes. Nucleic Acids Res. 2004;32:W615-W619.
23. Bruce LJ. Red cell membrane transport abnormalities. Curr Opin Hematol. 2008;15:184-190.
24. Tilley L, Gaskell A, Poole J, Daniels G. Duclos-negative and Ol(a+) blood group phenotypes are associated with amino acid substitutions in the external loops of the Rh-associated glycoprotein [abstract]. Vox Sang. 2008;95:37. Abstract 3C-S18-03.
25. Conroy MJ, Bullough PA, Merrick M, Avent ND. Modelling the human rhesus proteins: implications for structure and function. Br J Haematol. 2005;131:543-551.
26. Huang CH, Peng J. Evolutionary conservation and diversification of Rh family genes and proteins. Proc Natl Acad Sci U S A. 2005;102:15512-15517.

27. Marcus Y. Ion solvation. Chicester, UK: Wiley; 1985.
28. Hemker MB, Cheroutre G, van Zwieten R, et al. The Rh complex exports ammonium from human red blood cells. Br J Haematol. 2003;122:333-340.
29. Ripoche P, Bertrand O, Gane P, et al. Human Rhesus-associated glycoprotein mediates facilitated transport of NH(3) into red blood cells. Proc Natl Acad Sci U S A. 2004;101:17222-17227.
30. Benjelloun F, Bakouh N, Fritsch J, et al. Expression of the human erythroid Rh glycoprotein (RhAG) enhances both NH3 and NH4+ transport in HeLa cells. Pflugers Arch. 2005;450:155-167.
31. Marini AM, Matassi G, Raynal V, André B, Cartron JP, Chérif-Zahar B. The human Rhesus-associated RhAG protein and a kidney homologue promote ammonium transport in yeast. Nat Genet. 2000;26:341-344.
32. Westhoff CM, Wylie DE. Transport characteristics of mammalian Rh and Rh glycoproteins expressed in heterologous systems. Transfus Clin Biol. 2006;13:132-138.
33. Szekely D, Chapman BE, Bubb WA, Kuchel PW. Rapid exchange of fluoroethylamine via the Rhesus complex in human erythrocytes: 19F NMR magnetization transfer analysis showing competition by ammonia and ammonia analogues. Biochemistry. 2006;45:9354-9361.
34. Ripoche P, Goossens D, Devuyst O, et al. Role of RhAG and AQP1 in NH_3 and CO_2 gas transport in red cell ghosts: a stopped-flow analysis. Transfus Clin Biol. 2006;13:117-122.
35. Kustu S, Inwood W. Biological gas channels for NH3 and CO2: evidence that Rh (Rhesus) proteins are CO2 channels. Transfus Clin Biol. 2006; 13:103-110.
36. Endeward V, Cartron JP, Ripoche P, Gros G. RhAG protein of the Rhesus complex is a CO2 channel in the human red cell membrane. FASEB J. 2008;22:64-73.
37. Missner A, Kügler P, Saparov SM, et al. Carbon dioxide transport through membranes. J Biol Chem. 2008;283:25340-25347.
38. Fong RN, Kim K-S, Yoshihara C, Inwood WB, Kustu S. The W148L substitution in the Escherichia coli ammonium channel AmtB increases flux and indicates that the substrate is an ion. Proc Natl Acad Sci U S A. 2007;104:18706-18711.
39. Montel-Hagen A. Erythrocyte Glut1 triggers dehydroascorbic acid uptake in mammals unable to synthesize vitamin C. Cell. 2008;132:1039-1048.
40. Mentzer WC Jr, Smith WB, Goldstone J, Shohet SB. Hereditary stomatocytosis: membrane and metabolism studies. Blood. 1975;46:659-669.